



AFRL-AFOSR-VA-TR-2016-0165

(BRI) Microresonator-Based Optical Frequency Combs: A Time Domain Perspective

**Andrew Weiner
PURDUE UNIVERSITY
401 SOUTH GRANT ST
WEST LAFAYETTE, IN 47907-2024**

**04/19/2016
Final Report**

<p>DISTRIBUTION A: Distribution approved for public release.</p>

Air Force Research Laboratory
AF Office Of Scientific Research (AFOSR)/RTB1

Arlington, Virginia 22203
Air Force Materiel Command

DISTRIBUTION A: Distribution approved for public release.

REPORT DOCUMENTATION PAGE				<i>Form Approved</i> OMB No. 0704-0188		
<small>The public reporting burden for this collection of information is estimated to average 1 hour per response, including the time for reviewing instructions, searching existing data sources, gathering and maintaining the data needed, and completing and reviewing the collection of information. Send comments regarding this burden estimate or any other aspect of this collection of information, including suggestions for reducing the burden, to the Department of Defense, Executive Service Directorate (0704-0188). Respondents should be aware that notwithstanding any other provision of law, no person shall be subject to any penalty for failing to comply with a collection of information if it does not display a currently valid OMB control number.</small>						
PLEASE DO NOT RETURN YOUR FORM TO THE ABOVE ORGANIZATION.						
1. REPORT DATE (DD-MM-YYYY) 15-04-2016		2. REPORT TYPE Final		3. DATES COVERED (From - To) 01 JUL 2012 - 31 DEC 2015		
4. TITLE AND SUBTITLE Microresonator-Based Optical Frequency Combs: A Time Domain Perspective				5a. CONTRACT NUMBER		
				5b. GRANT NUMBER FA9550-12-1-0236		
				5c. PROGRAM ELEMENT NUMBER		
6. AUTHOR(S) Andrew M. Weiner				5d. PROJECT NUMBER		
				5e. TASK NUMBER		
				5f. WORK UNIT NUMBER		
7. PERFORMING ORGANIZATION NAME(S) AND ADDRESS(ES) PURDUE UNIVERSITY 401 SOUTH GRANT ST WEST LAFAYETTE IN 47907-2024				8. PERFORMING ORGANIZATION REPORT NUMBER		
9. SPONSORING/MONITORING AGENCY NAME(S) AND ADDRESS(ES) USAF, AFRL DUNS 143574726 AF OFFICE OF SCIENTIFIC RESEARCH 875 N. RANDOLPH ST. ROOM 3112 ARLINGTON VA 22203				10. SPONSOR/MONITOR'S ACRONYM(S)		
				11. SPONSOR/MONITOR'S REPORT NUMBER(S)		
12. DISTRIBUTION/AVAILABILITY STATEMENT Distribution A - Approved for Public Release						
13. SUPPLEMENTARY NOTES						
14. ABSTRACT Optical frequency combs are promising for a variety of applications. Comb generation based on nonlinear wave mixing in optical microresonators offers promise to replace traditional mode-locked laser combs and to substantially shrink the size of comb sources to the chip-level for applications outside of specialized research laboratories. In this project we studied comb generation in microresonators formed in silicon nitride films on silicon chips. Our most important contribution has been to convincingly demonstrate that in addition to the anomalous dispersion microresonator devices commonly studied, comb generation can and does occur in normal dispersion microresonators and is made possible by interactions between different spatial modes in the few-moded waveguides from which the microresonators are fabricated. Time domain measurements show for the first time that under normal dispersion, combs can take the form of mode-locked dark pulses. Comb generation from normal dispersion microresonators offers potential for operation deep into the visible spectrum (where normal dispersion dominates), may be compatible with thinner, lower loss films, and may provide opportunities for higher power (at the cost of reduced optical bandwidth).						
15. SUBJECT TERMS optical frequency combs; photonics; microresonators; nonlinear optics; ultrafast optics						
16. SECURITY CLASSIFICATION OF: a. REPORT b. ABSTRACT c. THIS PAGE			17. LIMITATION OF ABSTRACT	18. NUMBER OF PAGES	19a. NAME OF RESPONSIBLE PERSON 19b. TELEPHONE NUMBER (Include area code)	

INSTRUCTIONS FOR COMPLETING SF 298

1. REPORT DATE. Full publication date, including day, month, if available. Must cite at least the year and be Year 2000 compliant, e.g. 30-06-1998; xx-06-1998; xx-xx-1998.

2. REPORT TYPE. State the type of report, such as final, technical, interim, memorandum, master's thesis, progress, quarterly, research, special, group study, etc.

3. DATES COVERED. Indicate the time during which the work was performed and the report was written, e.g., Jun 1997 - Jun 1998; 1-10 Jun 1996; May - Nov 1998; Nov 1998.

4. TITLE. Enter title and subtitle with volume number and part number, if applicable. On classified documents, enter the title classification in parentheses.

5a. CONTRACT NUMBER. Enter all contract numbers as they appear in the report, e.g. F33615-86-C-5169.

5b. GRANT NUMBER. Enter all grant numbers as they appear in the report, e.g. AFOSR-82-1234.

5c. PROGRAM ELEMENT NUMBER. Enter all program element numbers as they appear in the report, e.g. 61101A.

5d. PROJECT NUMBER. Enter all project numbers as they appear in the report, e.g. 1F665702D1257; ILIR.

5e. TASK NUMBER. Enter all task numbers as they appear in the report, e.g. 05; RF0330201; T4112.

5f. WORK UNIT NUMBER. Enter all work unit numbers as they appear in the report, e.g. 001; AFAPL30480105.

6. AUTHOR(S). Enter name(s) of person(s) responsible for writing the report, performing the research, or credited with the content of the report. The form of entry is the last name, first name, middle initial, and additional qualifiers separated by commas, e.g. Smith, Richard, J, Jr.

7. PERFORMING ORGANIZATION NAME(S) AND ADDRESS(ES). Self-explanatory.

8. PERFORMING ORGANIZATION REPORT NUMBER. Enter all unique alphanumeric report numbers assigned by the performing organization, e.g. BRL-1234; AFWL-TR-85-4017-Vol-21-PT-2.

9. SPONSORING/MONITORING AGENCY NAME(S) AND ADDRESS(ES). Enter the name and address of the organization(s) financially responsible for and monitoring the work.

10. SPONSOR/MONITOR'S ACRONYM(S). Enter, if available, e.g. BRL, ARDEC, NADC.

11. SPONSOR/MONITOR'S REPORT NUMBER(S). Enter report number as assigned by the sponsoring/monitoring agency, if available, e.g. BRL-TR-829; -215.

12. DISTRIBUTION/AVAILABILITY STATEMENT. Use agency-mandated availability statements to indicate the public availability or distribution limitations of the report. If additional limitations/ restrictions or special markings are indicated, follow agency authorization procedures, e.g. RD/FRD, PROPIN, ITAR, etc. Include copyright information.

13. SUPPLEMENTARY NOTES. Enter information not included elsewhere such as: prepared in cooperation with; translation of; report supersedes; old edition number, etc.

14. ABSTRACT. A brief (approximately 200 words) factual summary of the most significant information.

15. SUBJECT TERMS. Key words or phrases identifying major concepts in the report.

16. SECURITY CLASSIFICATION. Enter security classification in accordance with security classification regulations, e.g. U, C, S, etc. If this form contains classified information, stamp classification level on the top and bottom of this page.

17. LIMITATION OF ABSTRACT. This block must be completed to assign a distribution limitation to the abstract. Enter UU (Unclassified Unlimited) or SAR (Same as Report). An entry in this block is necessary if the abstract is to be limited.

Microresonator-Based Optical Frequency Combs: A Time Domain Perspective

Contract/Grant #: FA9550-12-1-0236

Prof. Andrew M. Weiner
Scifres Family Distinguished Professor of Electrical and Computer Engineering, Purdue University
phone: 765-494-5574
email: amw@purdue.edu
web: <https://engineering.purdue.edu/~amw/>

1. Introduction

Optical frequency comb generation via nonlinear wave mixing in high quality factor microresonators is now a very active research topic. Our group's initial contribution, prior to the onset of this grant, was to report the initial time domain investigations of such combs. Working in a chip-based silicon nitride platform, we showed for the first time that by employing line-by-line pulse shaping, compression into transform-limited pulses could be achieved [1]. Furthermore, our time-domain pulse compression experiments were the first to reveal differences in coherence properties associated with different pathways to comb formation. Our findings stimulated substantial effort by many groups, our own included, to understand the mechanisms responsible for high and low coherence combs, to elucidate different modes of nonlinear operation, and find ways to guide the system to the high coherence operation needed for most applications.

Under this grant our team at Purdue has made substantial progress, both in advancing the technology and in unraveling new physics that elucidates aspects of the complicated, nonlinear comb generation process. In the following I briefly summarize some of our progress, findings, and accomplishments (section 2) and then discuss two important examples of research in more detail (sections 3 and 4).

2. Research progress, findings, and accomplishments

- 1) We followed up our discovery of different routes to comb formation leading to different optical coherence behavior by showing that in cases when it is degraded, the coherence varies within the comb spectrum in a way that is related to the route to comb formation. We also showed that optical coherence, intensity noise, and lightwave communications performance are correlated, suggesting the relevance of optical coherence to practical applications [2, 3].
- 2) We achieved combs with devices fabricated at Purdue. (Previously we had studied microrings from collaborators at NIST.) Furthermore, we have substantially improved device quality and design flexibility, which are important both for achieving desirable performance and for probing the nonlinear physics. Some examples of our accomplishments include: (a) We have learned how to grow crack-free SiN films at 800 nm thickness. This allows us to reach the anomalous dispersion regime; thinner films yield waveguides with normal dispersion. Dispersion (and its sign) is usually viewed as crucial in the comb generation process; we are now in a position to compare and contrast microresonators with both signs of dispersion. (b) Previously our combs had spacings of 115 GHz and above. Consistent with the goals of this program, we have now realized microresonators at 75, 37.5, and 25 GHz free spectral range (FSR) and have observed comb generation at frequency spacings down to 25 GHz, in the range where convenient electronic detection is possible. (c) Our best Purdue microrings had quality factors (Q's) around 10^6 at start of program. We have now observed examples of microrings with intrinsic Q's as high as 1.7×10^7 at a 25 GHz FSR. These are the highest

Q's reported for chip-scale microring resonators capable of generating combs. This has the impact of dramatically lowering required optical pump powers and can open the door to integration or co-assembly of microresonator comb sources with compact, photonic integrated circuit pump lasers.

An important point is that the chip-based SiN platform allows device fabrication via powerful microlithography techniques. This allows fabrication of many devices features and even new structures that are very useful in probing the nonlinear comb physics, e.g., drop ports, microheaters that provide a new tuning mechanism to help steer the nonlinear dynamics, coupled rings, etc.

- 3) We have fabricated microrings in a drop port geometry; this provides access to the comb spectrum without the complication of a much stronger, overlapping pump line that plagues the conventional through port geometry. As a result we have obtained new data on pump saturation and power transfer to the comb as well as a first observation of mode-locked pulses without the need to filter out the pump [4].
- 4) Much of the discussion on microcomb generation invokes the modulational instability as the comb starting mechanism and assumes anomalous group velocity dispersion (which is required for the modulational instability in conventional nonlinear fiber optics). **Some leading groups have stated that anomalous dispersion is required for comb generation. We now have clear evidence that refutes such claims and shows generation of stable, coherent combs both from normal dispersion microrings and from anomalous dispersion microrings.** We also have evidence of new routes to comb generation applicable for normal dispersion microrings along with observations of novel dark pulse time domain waveforms [5]. More details are provided in Section 3.
- 5) Most microresonators used for comb generation, including the SiN microrings used in our work, are not single-moded. "Few-moded" is a more accurate description. This raises a question: what role if any do interactions between different transverse modes play in the comb generation. **We have performed precision transmission spectroscopy of SiN microresonators, providing the first definitive evidence of strong interactions between different transverse modes in these multimode waveguides. Further data demonstrate such interactions play a major role in the generation of combs, especially for normal dispersion devices [6].** More details are provided in Section 4.

3. Understanding micro-comb waveforms and nonlinear dynamics: observation of mode-locked dark pulses

It has become clear that micro-comb generation features many different nonlinear operating regimes, that there is a large nonlinear phase space, and that in many cases micro-comb operation depends not only on the current parameter settings (pump power, phase detuning, etc.) but also on their history. In some cases a coherent comb is generated directly at single FSR spacing (a Type I comb); in other cases the comb is generated at multiple-FSR spacing and later fills in to yield approximately single-FSR spacing but with multiple noncommensurate subcombs characterized by low coherence and high intensity noise (a Type II comb) [1, 7]. With proper sequence of power and laser frequency tuning, Type II combs sometimes collapse into a mode-locked state characterized by low intensity noise, high coherence, and soliton-like pulses within the microresonator. Previously such operation was observed only in the anomalous dispersion regime [8, 9]. Under this grant we have observed mode-locking behavior in SiN microresonators. To our knowledge we are the **first to make any observation of such mode-locking in the normal dispersion regime.** Unlike the previous results in the anomalous dispersion regimes, our waveforms do not appear to be particularly pulse-like within the microresonator - but they are fully compressible after compensating the spectral phase with an external pulse shaper.

In the following I summarize some of our results on mode-locking with a normal dispersion microring device [5] – see Fig. 1. Figure 1(a) shows the experimental setup and a photo of the microring, which is fabricated with a resistive heater. The heater allows us to tune the resonance frequencies independently of the laser power and tuning; the extra degree of freedom has proved to be very convenient to access new comb phenomena. Figure 1(b) demonstrates tuning of the comb offset frequency – a central concept in frequency combs – achieved by adjusting the laser frequency and microheater voltage simultaneously. Fifteen traces are overlaid, showing for the first time to our knowledge that the absolute frequency of a comb line can be tuned over nearly the full FSR while maintaining the same regime of comb operation. Figure 1(c) shows optical and RF spectra as the resonance detuning is changed via the microheater. The first row shows an early stage in comb development, in which clusters of comb lines surround the initial comb sidebands, spaced by ~ 100 nm. The comb is accompanied by broadband intensity noise. With additional tuning into resonance (second row), the comb spectrum fills in to yield a single FSR comb, still with intensity noise but now appearing as a narrow noise peak around 700 MHz. The narrow RF peak signifies quasi-periodic slow evolution of the comb, often termed a “breather.” The combs of the first and second rows cannot be compressed and are therefore incoherent. With still more tuning into resonance (third row), the intensity noise drops down to the instrumental limit. This is a mode-locking transition, observed here for the first time in the normal dispersion regime. Although the comb is **not** a pulse inside the microring, by compensating the comb’s frequency dependent phase with an external pulse shaper, we can compress the comb output to the bandwidth limit, realizing exceptionally clean trains of pulses ~ 318 fs in duration (Fig. 1(d)). Note that Fig. 1(d) overlaps autocorrelations for all 15 comb traces from Fig. 1(b); clearly coherent mode-locking operation is maintained as the comb is tuned. Figure 1(e) shows several examples of the frequency dependent phase for different pump wavelengths and even on different days (these are extracted from the phases applied to the pulse shaper in order to get the best compression). Clearly the combs have a strong but reproducible spectral phase variation. By using the spectral phase variation of Fig. 1(e) together with the comb power spectrum, we can compute the complex electric field of the comb internal to the microring, Fig. 1(f). The comb takes the shape of a dark pulse, consisting of a transient, rectangular shaped dip in the intensity with sharp edges. A significant temporal phase variation, corresponding to modulation of the instantaneous frequency, is also present. Although recently predicted in simulation papers [10], such dark pulse time domain waveforms have not been observed previously in comb generation. Finally, by performing simulations with carefully chosen initial conditions, we can obtain waveforms similar to those observed experimentally, Fig. 1(g). The intensity vs. fast time evidently takes the form of a dark pulse. The slow time axis captures the transient evolution of the comb. Here we initially choose parameters yielding quasi-periodic evolution of the comb waveform, corresponding to the breather of Fig. 1(c). The breather evolves into a stable dark pulse when the pump power is reduced around a normalized time of 40. Thus, through simulation we can not only find solutions that closely resemble the observed mode-locked state, but we can also gain insight into some of the stages of comb development that precede the mode-locking.

I have not yet discussed how combs from normal dispersion microrings, such as those of Fig. 1, are initiated. We have strong evidence that the comb initiation is strongly linked to interactions between transverse waveguide modes, which shift resonance frequencies in the interacting spectral region. This may strongly affect the local dispersion, even changing its sign. Such mode interaction effects are discussed below in Section 4.

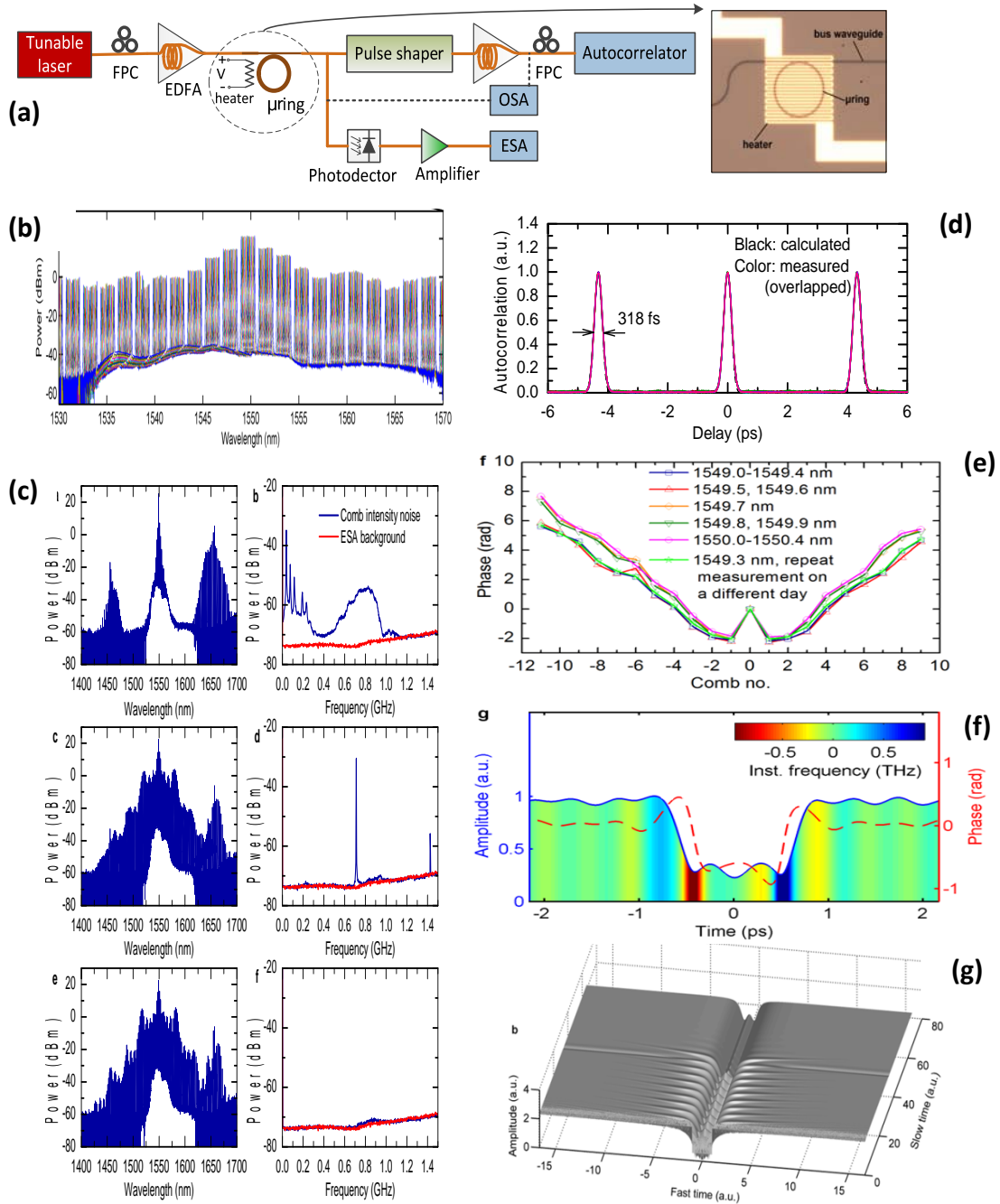


Fig. 1. Mode-locking with normal dispersion microring. (a) Experimental layout and microring with overlaid heater. (b) Comb spectra, selected to span the lightwave C band; 15 overlaid traces demonstrate tuning of the comb offset frequency. (c) Variation of comb optical spectrum and RF intensity noise spectrum as system is tuned (top to bottom) into resonance; mode-locking transition is observed in bottom row. (d) Overlaid autocorrelations of 15 spectra from part (b) after compression via spectral phase shaping. (e) Spectral phase profiles extracted from optimum pulse shaper settings. (f) Computed temporal waveform internal to the microring. (g) Simulation results that reproduce key aspects of the experimental observations.

4. Mode interactions

We have often observed – particularly for normal dispersion microrings – that the same physical microresonator can show drastically different comb generation behavior when the pump is tuned by just a few free spectral ranges to access different resonant modes. The changes in the generated combs appear to be too large to plausibly explain based on small changes in dispersion. We now understand these observations are largely explained by the transverse mode content. The simple picture that characterizes the resonator modes by a single free spectral range is only adequate for a single-mode waveguide. Low-loss SiN microrings are usually characterized by few mode waveguides. Microtoroid and microsphere-based systems support multiple transverse mode families as well – each with a distinct mode spacing. Under this grant we have made important progress in observing mode interaction effects both in linear and nonlinear optics, which we summarize below [6].

We can illustrate mode interaction effects by using coupled mode theory to simulate a system of two coupled resonant modes. Resulting transmission spectra are plotted for different separations (over the range -5 GHz to 5 GHz) between the resonances of the two modes. Without mode coupling (Fig. 2(a)), the resonances approach and cross each other at a constant rate. However, with mode coupling turned on with a strength picked to match an experiment presented below, the dips in transmission are shifted in frequency, resulting in an avoided crossing (Fig. 2(b)). The mode interactions also lead to significant changes in the extinction ratios and linewidths of the resonant features.

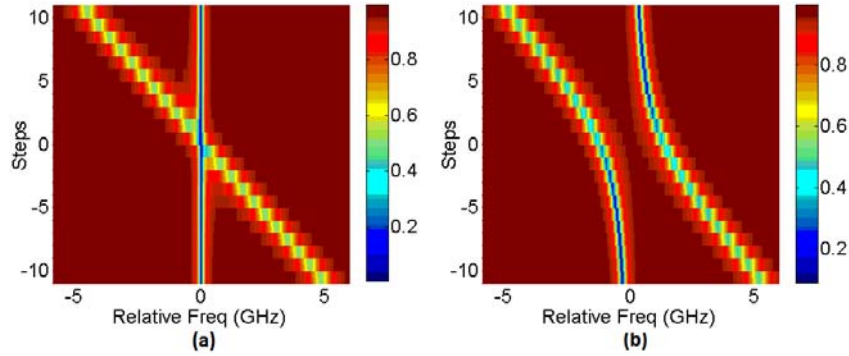


Fig. 2 Numerical investigation of mode coupling effect when the resonances of the two modes get close and cross each other. (a) transmission spectra with no mode coupling; (b) transmission spectra with mode coupling.

Similar effects are observed in experiments. In one study, we investigated silicon nitride resonators fabricated to have $2\ \mu\text{m} \times 550\ \text{nm}$ waveguide cross-section. According to simulation for the two transverse electric (TE) modes, TE_1 and TE_2 , these waveguides are clearly in the normal dispersion regime with $D \sim -156\ \text{ps/nm} \cdot \text{km}$ and $D \sim -160\ \text{ps/nm} \cdot \text{km}$ respectively [4]. Figure 3(a) shows an image of a resonator with a total path length of 5.92 mm which corresponds to a FSR slightly under 25 GHz. The light is coupled both in and out through lensed fibers which are positioned in U-grooves to improve stability when working at high power [4]. The measured transmission spectrum, showing resonances throughout the lightwave C band, is given in Fig. 3(b). If we zoom in the transmission spectrum as shown in the inset, resonances of 2 transverse mode families with different depth can be observed. The loaded Q factors at the frequencies shown are ca. 1×10^6 (intrinsic $Q \sim 1.7 \times 10^6$) and 0.3×10^6 (intrinsic $Q \sim 0.35 \times 10^6$) for modes 1 and 2, respectively. We use the frequency-comb-assisted spectroscopy method of [11] to accurately determine the resonance positions and compute the changes in free spectral range (FSR) with wavelength to estimate the dispersion for TE modes. The measured FSRs are given in Fig. 4(a). The FSRs for the two modes are around 24.8 GHz and 24.4 GHz, respectively. Both modes are fitted with our simulated dispersion showing good accordance which confirms that the resonator is in the normal dispersion regime for TE modes. However, at several wavelengths for which

the resonances associated with the two transverse modes are closely spaced (1532 nm, 1542 nm and 1562 nm), the FSRs of the two modes change significantly, such that their FSRs become more similar. In these cases we clearly observe that the mode coupling results in a major modification to the local dispersion, even changing the sign of dispersion in some wavelength regions. To take a closer look at this phenomenon, in Fig. 4(b) we plot the transmission spectrum in the vicinity of the mode crossing region near 1542 nm. To visualize the data in a form analogous to the simulations of Fig. 2, we vertically align different pieces of the transmission spectrum separated by a constant 24.82 GHz increment (the nominal FSR of the higher Q mode around 1542 nm). Since the average dispersion contributes a change in FSR below 15 MHz in the range plotted without mode coupling, one of the modes should appear as very nearly a vertical line, while the other should appear as a tilted line due to the difference in FSRs. However in Fig. 4(b), we observe that the curves bend as they approach each other, resulting in an avoided crossing, quite similar to the simulation results of Fig. 2(b). These data provide detailed and compelling evidence of strong mode coupling effects on the linear spectrum and are closely analogous to avoided crossings that are well known in studies of quantum mechanical energy surfaces.

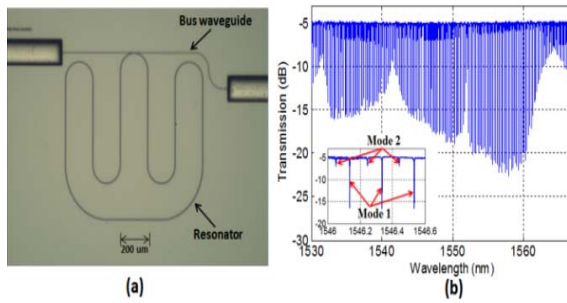


Fig. 3. (a) Microscope image of silicon nitride resonator with path length of 5.92 mm. (b) Measured transmission spectrum of the resonator. Inset is the zoom-in transmission spectrum showing resonances from different transverse mode families.

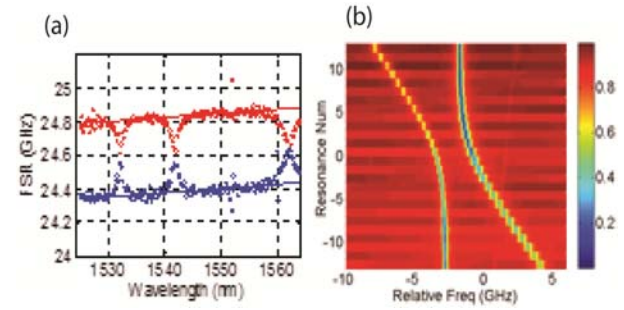


Fig. 4. (a) Measured FSR vs. wavelength for two TE modes, plotted in red and blue and fitted with $D \sim -156 \text{ ps/nm} \cdot \text{km}$ and $D \sim -160 \text{ ps/nm} \cdot \text{km}$, respectively. (b) Aligned resonances with fixed increment for strongly coupled mode at 1542 nm, showing clear avoided crossing.

A practical impact is that the value of the dispersion (D) changes from around -156 ps/nm/km to over 5000 ps/nm/km close to the strongest avoided crossing of Fig. 4(a). Not only does the magnitude increase by more than a decade, but also the sign changes from normal to anomalous. We have shown that this effect may play a strong and helpful role in initiation of combs from normal dispersion microresonators. This is in contrast to recent reports from other groups on mode interactions in anomalous dispersion microresonators, where such interactions are considered detrimental and may even inhibit comb formation [12, 13]. In comb generation experiments, we pumped the micro-resonator with a single CW tuned to different resonances of the high-Q mode family and recorded the comb spectra. The results are given in Fig. 5(a). We pump at 28 different resonances between 1554 and 1560 nm. The frequency spacing of the comb varies from 33 FSR for pumping at 1554 nm to 7 FSR for pumping at 1559.4 nm. We observe that the nearest long wavelength sideband remains anchored at approximately 1560.5 nm, very close to the $\sim 1562 \text{ nm}$ mode interaction feature. With the pump shifted by a total of 694 GHz (27 FSRs), we find that the long wavelength sideband varies by no more than $\pm 25 \text{ GHz}$ ($\pm 1 \text{ FSR}$). Meanwhile the short wavelength sideband varies at twice the rate of the pump tuning, for a total frequency variation of $\sim 1.3 \text{ THz}$. Similar pinning of an initial sideband has also been observed at the other strong mode interaction regions (1532 nm, 1542 nm), but for a smaller number of pump wavelengths. (The different mode interaction features may compete with each other in initializing the combs.) The observed pinning of one of the initial sidebands very close to a mode interaction feature clearly suggests that mode coupling is a major factor in comb initiation in this normal dispersion microresonator. We may understand this behavior simply as follows: frequency shift of a specific

resonance due to mode coupling introduces an effective per round trip phase shift for the component of the light field at that resonance. If the sign of the phase shift is correct and its amplitude sufficient, this mimics the effect of anomalous dispersion to provide a modulational instability effect that amplifies small fluctuations of the initial light field at the affected optical frequency.

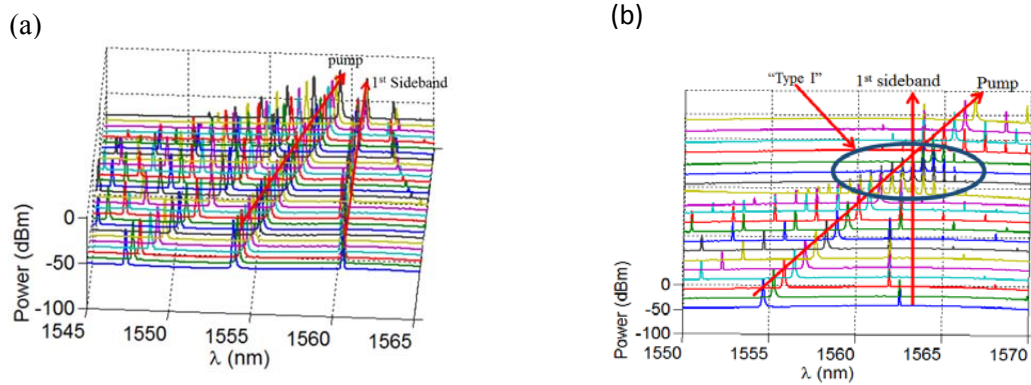


Fig. 5. Comb generation at different pump wavelengths with one of the 1st sidebands pinned at an approximately constant location. (a) ~25 GHz FSR resonator, pinning at ~1560 nm. (b) ~75 GHz resonator, pinning at ~1563 nm.

Such effects appear to provide a much sought after means for forcing comb generation with an initial 1-FSR spacing, a formula that leads to coherent combs from the outset. In contrast, for large devices with FSRs in the tens of GHz regime, the amount of (anomalous) dispersion needed for favor a single-FSR route to comb generation is usually believed to be impractically large.

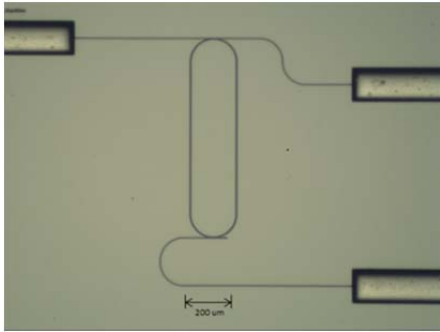


Fig. 6. Image of ~75 GHz FSR resonator fabricated with drop port. U groove structures for fiber coupling are also shown.

We have observed such operation in experiments with a similar but somewhat smaller normal dispersion SiN resonator with FSR slightly below 75 GHz. As shown in Fig. 6, this resonator also has a drop-port which has been observed to reduce the power difference between the pump and adjacent comb lines, yielding a smoother comb spectrum without the usual strong pump background [4]. Using the frequency-comb-assisted spectroscopy method, two mode families with FSRs around 74.7 GHz and 72 GHz are observed, with a strong avoided crossing due to mode interaction are 1563 nm. The comb results are shown in Fig. 5(b) for pumping between 1554.71 nm and 1566.59 nm. Again one of the 1st sidebands is “pinned” near the mode crossing wavelength. Although the first sideband has a 13-FSR separation when pumping at 1555 nm, the desired single-FSR comb can be generated for pumping at 1562.62 nm, 1563.22 nm, 1563.81 and 1564.43 nm (as shown in the circled area). As an example, pumping at 1562.62 nm at higher power, more than 20 comb lines with 1 FSR separation are generated. The spectrum observed at the drop port is shown in Fig. 7(a). Fifteen of the lines are selected by a bandpass filter and amplified in an EDFA; the resulting spectrum is shown in Fig. 7(b). The amplified and filtered comb is directed (through a carefully dispersion compensated fiber link) to an intensity autocorrelator. The autocorrelation trace measured for the comb is plotted in Fig. 7(c). Also plotted is the autocorrelation of the ideal bandwidth-limited pulse, calculated from the spectrum of Fig. 7(b) with the assumption of flat phase. Clearly the generated pulses, with estimated duration of 2.7 ps FWHM, are very close to bandwidth-limited. We have also used a photodetector and spectrum analyzer to look at the

low frequency intensity noise of the comb, Fig. 7(d)). The intensity noise is below the background level of our measurement setup. Similar low noise, bandwidth-limited pulse generation is observed for the single-FSR combs generated via pumping at other resonances of this same resonator. These data demonstrate that the single-FSR combs reported here are generated *directly* in a mode-locked state featuring low noise, high coherence, and bandwidth-limited temporal profile, though with a limited number of comb lines.

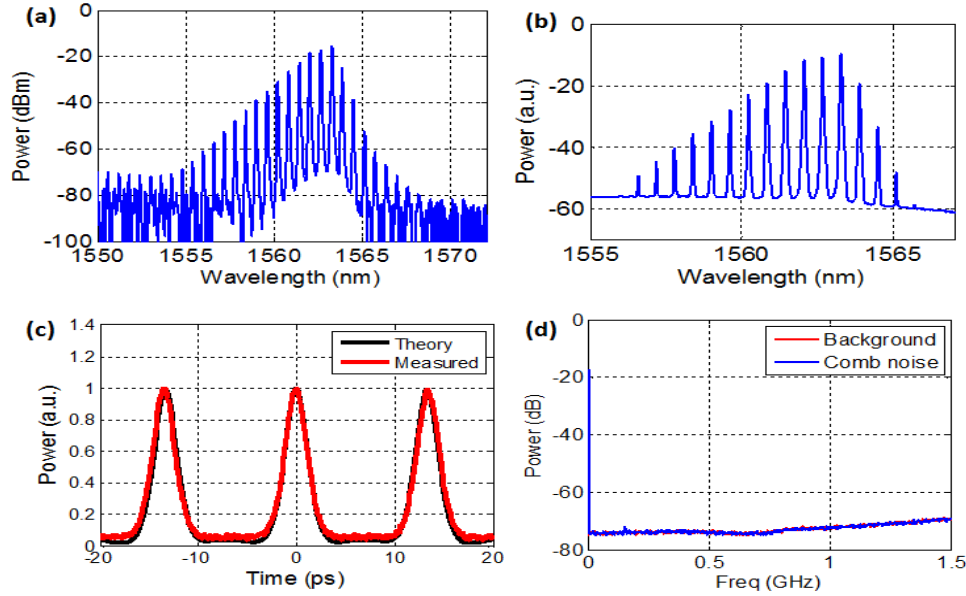


Fig. 7. Generation of coherent mode-locked single-FSR comb due to mode coupling. (a) Generated comb spectrum at the drop port. (b) 15 lines are selected, amplified and filtered for time-domain characterization. (c) Autocorrelation trace compared with that of theoretical bandwidth-limited pulse, showing good coherence and mode locking behavior. (d) Intensity noise at the measurement system noise floor.

The key points in this section are summarized as follows: (1) We have observed strong evidence of mode interactions, manifested in clear shifts of the resonant frequencies when two different transverse mode families are close in frequency. Transmission spectra plots can be formatted to beautifully show avoided crossings. (2) These resonance frequency shifts modify the frequency dependence of the FSR, which is equivalent to modifying the dispersion, and can be very large: a microring constructed from a normal dispersion microring can exhibit local anomalous dispersion in the vicinity of a mode crossing. (3) Such effects have important consequences, especially for normal dispersion devices, including anchoring of an initial sideband at a mode interaction region and (in some cases) generation of single-FSR combs directly as coherent, bandwidth-limited pulses without the need to undergo a later mode-locking transition. Such mode interaction effects also play a key role in normal dispersion devices in initiation of combs that later transition into mode-locked dark pulses, such as those in Fig. 1.

5. References

- [1] F. Ferdous, H. Miao, D. E. Leaird, K. Srinivasan, J. Wang, L. Chen, *et al.*, "Spectral line-by-line pulse shaping of on-chip microresonator frequency combs," *Nature Photonics*, vol. 5, pp. 770-776, 2011.
- [2] F. Ferdous, H. Miao, P.-H. Wang, D. E. Leaird, K. Srinivasan, L. Chen, *et al.*, "Probing coherence in microcavity frequency combs via optical pulse shaping," *Opt. Express*, vol. 20, pp. 21033-21043, 2012.
- [3] P. H. Wang, F. Ferdous, H. X. Miao, J. Wang, D. E. Leaird, K. Srinivasan, *et al.*, "Observation of correlation between route to formation, coherence, noise, and communication performance of Kerr combs," *Optics Express*, vol. 20, pp. 29284-29295, Dec 2012.
- [4] P. H. Wang, Y. Xuan, L. Fan, L. T. Varghese, J. Wang, Y. Liu, *et al.*, "Drop-port study of microresonator frequency combs: power transfer, spectra and time-domain characterization," *Optics Express*, vol. 21, pp. 22441-22452, Sep 2013.
- [5] X. Xue, Y. Xuan, Y. Liu, P.-H. Wang, S. Chen, J. Wang, *et al.*, "Mode-locked dark pulse Kerr combs in normal-dispersion microresonators," *Nature Photonics* **9**, 594-600 (2015)..
- [6] Y. Liu, Y. Xuan, X. Xue, P.-H. Wang, S. Chen, A. J. Metcalf, *et al.*, "Investigation of Mode Coupling in Normal Dispersion Silicon Nitride Microresonators for Kerr Frequency Comb Generation " *Optica*, vol. 1, pp. 137-144, 2014.
- [7] T. Herr, K. Hartinger, J. Riemensberger, C. Y. Wang, E. Gavartin, R. Holzwarth, *et al.*, "Universal formation dynamics and noise of Kerr-frequency combs in microresonators," *Nature Photonics*, vol. 6, pp. 480-487, Jul 2012.
- [8] K. Saha, Y. Okawachi, B. Shim, J. S. Levy, R. Salem, A. R. Johnson, *et al.*, "Modelocking and femtosecond pulse generation in chip-based frequency combs," *Optics Express*, vol. 21, pp. 1335-1343, Jan 2013.
- [9] T. Herr, V. Brasch, J. D. Jost, C. Y. Wang, N. M. Kondratiev, M. L. Gorodetsky, *et al.*, "Temporal solitons in optical microresonators," *Nature Photonics*, vol. 8, pp. 145-152, Feb 2014.
- [10] A. Coillet, I. Balakireva, R. Henriet, K. Saleh, L. Larger, J. M. Dudley, *et al.*, "Azimuthal Turing Patterns, Bright and Dark Cavity Solitons in Kerr Combs Generated With Whispering-Gallery-Mode Resonators," *Ieee Photonics Journal*, vol. 5, Aug 2013.
- [11] P. Del'Haye, O. Arcizet, M. L. Gorodetsky, R. Holzwarth, and T. J. Kippenberg, "Frequency comb assisted diode laser spectroscopy for measurement of microcavity dispersion," *Nature Photonics*, vol. 3, pp. 529-533, Sep 2009.
- [12] I. S. Grudinin, L. Baumgartel, and N. Yu, "Impact of cavity spectrum on span in microresonator frequency combs," *Optics Express*, vol. 21, pp. 26929-26935, Nov 2013.
- [13] T. Herr, V. Brasch, J. D. Jost, I. Mirgorodskiy, G. Lihachev, M. L. Gorodetsky, *et al.*, " Mode spectrum and temporal soliton formation in optical microresonators," *Physical review letters*, **113**(12), 123901 (2014).

1.

1. Report Type

Final Report

Primary Contact E-mail**Contact email if there is a problem with the report.**

amw@purdue.edu

Primary Contact Phone Number**Contact phone number if there is a problem with the report**

7654945574

Organization / Institution name

Purdue University

Grant/Contract Title**The full title of the funded effort.**

Microresonator-Based Optical Frequency Combs: A Time Domain Perspective

Grant/Contract Number**AFOSR assigned control number. It must begin with "FA9550" or "F49620" or "FA2386".**

FA9550-12-1-0236

Principal Investigator Name**The full name of the principal investigator on the grant or contract.**

Andrew Weiner

Program Manager**The AFOSR Program Manager currently assigned to the award**

Enrique Parra

Reporting Period Start Date

07/01/2012

Reporting Period End Date

12/31/2015

Abstract

Optical frequency combs, consisting of a multitude of evenly spaced optical frequency components that are locked together in phase, are promising for a variety of applications, including optical frequency metrology and frequency synthesis, low noise radio-frequency signal generation, optical arbitrary waveform generation, lightwave communications, spectroscopic sensing, and radio-frequency signal processing. Usually such combs are generated from stabilized mode-locked lasers. Within the last decade, alternative comb generation methods based on nonlinear optical modulation in high quality factor optical microresonators have been demonstrated, where pump photons are transformed into sideband photons in a four wave mixing process. This approach offers a potential way to substantially shrink the size of optical frequency comb sources to the chip-level to support applications outside of specialized research laboratories. However, understanding of the mechanisms for initiating combs from optical microresonators and steering them into desirable, low noise operation regimes has been lacking. In this project we have studied comb generation in microresonators formed in silicon nitride films on silicon chips. Generally, comb formation has been explained in terms of the interplay between nonlinear refractive index and group velocity dispersion. In anomalous dispersion microresonator devices, comb formation can be explained on the basis of a well known instability that is also operative in optical fibers. However, for fibers with normal group velocity dispersion, this instability does not occur; consequently, most researchers believed that

DISTRIBUTION A: Distribution approved for public release.

comb generation was not possible in normal dispersion microresonators. Our most important contribution in this project has been to convincingly demonstrate that comb generation can and does occur in normal dispersion microresonators. We have shown that such comb generation in normal dispersion microresonators is made possible by interactions between different spatial modes in the few-moded waveguides from which the microresonators are usually fabricated. We have also introduced new, dual-coupled on-chip microresonator structures that provide for tunable mode interactions for more dependable comb initiation. Comb generation from normal dispersion microresonators offers potential for comb operation deep into the visible spectrum (where normal dispersion dominates), may be compatible with thinner, lower loss films, and may provide opportunities for higher power, traded off against the wider bandwidth obtained with anomalous dispersion microresonators. In other aspects of our work, we have performed time domain measurements of the generated combs, leading to observation of novel, ultrafast dark pulse waveforms, have introduced new structures such as drop ports and thermo-optic tuners for integrated comb generation, and have achieved the lowest loss (highest quality factor) microresonators yet demonstrated in the silicon nitride material platform.

Distribution Statement

This is block 12 on the SF298 form.

Distribution A - Approved for Public Release

Explanation for Distribution Statement

If this is not approved for public release, please provide a short explanation. E.g., contains proprietary information.

SF298 Form

Please attach your SF298 form. A blank SF298 can be found [here](#). Please do not password protect or secure the PDF. The maximum file size for an SF298 is 50MB.

[SF298.pdf](#)

Upload the Report Document. File must be a PDF. Please do not password protect or secure the PDF. The maximum file size for the Report Document is 50MB.

[Final report main body.pdf](#)

Upload a Report Document, if any. The maximum file size for the Report Document is 50MB.

Archival Publications (published) during reporting period:

F. Ferdous, H. Miao, P.-H. Wang, D. E. Leaird, K. Srinivasan, L. Chen, V. Aksyuk, and A. M. Weiner, "Probing Coherence in Microcavity Frequency Combs via Optical Pulse Shaping," *Optics Express* 20, 21033-21043 (2012).
doi: 10.1364/OE.20.021033

P.-H. Wang, F. Ferdous, H. Miao, J. Wang, D. Leaird, K. Srinivasan, L. Chen, V. Aksyuk and A. M. Weiner, "Observation of correlation between route to formation, coherence, noise, and communication performance of Kerr combs," *Optics Express* 20, 29284-29295 (2012). doi: 10.1364/OE.20.029284

P.-H. Wang, Y. Xuan, L. Fan, L. Varghese, J. Wang, Y. Liu, X. Xue, D. E. Leaird, M. Qi, and A. M. Weiner, "Drop-Port Study of Microresonator Frequency Combs: Power Transfer, Spectra and Time-Domain Characterization," *Optics Express* 21, 22441-22452 (2013).
doi: 10.1364/OE.21.022441

P.-H. Wang, Y. Xuan, L. Fan, L. Varghese, J. Wang, Y. Liu, X. Xue, D. E. Leaird, M. Qi, and A. M. Weiner, "Drop-Port Study of Microresonator Frequency Combs: Power Transfer, Spectra and Time-Domain Characterization erratum," *Optics Express* 22, 12148-12148 (2014).
doi: 10.1364/OE.22.012148

Y. Liu, Y. Xuan, X. Xue, P.-H. Wang, S. Chen, A.J. Metcalf, J. Wang, D.E. Leaird, M. Qi, and A.M. Weiner, "Investigation of Mode Coupling in Normal Dispersion Silicon Nitride Microresonators for Kerr Frequency Comb Generation," *Optica* 1, 137-144 (2014).

DISTRIBUTION A: Distribution approved for public release.

doi: 10.1364/OPTICA.1.000137

X. Xue, Y.i Xuan, H.-J. Kim, J. Wang, D.E. Leaird, M. Qi, and A.M. Weiner, "Programmable Single-Bandpass Photonic RF Filter Based on Kerr Comb from a Microring," J. Lightwave Technol. 32, 3557-3565 (2014).
doi: 10.1109/JLT.2014.2312359

J.A. Jaramillo-Villegas, X. Xue, P.-H. Wang, D.E. Leaird, and A.M. Weiner, "Deterministic single soliton generation and compression in microring resonators avoiding the chaotic region." Optics Express 23, 9618-9626 (2015).
doi: 10.1364/OE.23.009618

X. Xue, Y. Xuan, Y. Liu, P.-H. Wang, S. Chen, J. Wang, D.E. Leaird, M. Qi, and A.M. Weiner, "Mode-locked dark pulse Kerr combs in normal-dispersion microresonators," Nature Photonics 9, 594-600 (2015).
doi: 10.1038/nphoton.2015.137

X. Xue, Y. Xuan, P.-H. Wang, Y. Liu, D.E. Leaird, M. Qi, and A.M. Weiner, "Normal-dispersion Microcombs Enabled by Controllable Mode Interactions," Laser & Photonics Reviews 9 (4), L23-L28 (2015).
DOI: 10.1002/lpor.201500107

Changes in research objectives (if any):

Not applicable

Change in AFOSR Program Manager, if any:

Not applicable

Extensions granted or milestones slipped, if any:

The program period includes a six month no-cost extension, which increased the grant period from 36 months to 42 months.

AFOSR LRIR Number

LRIR Title

Reporting Period

Laboratory Task Manager

Program Officer

Research Objectives

Technical Summary

Funding Summary by Cost Category (by FY, \$K)

	Starting FY	FY+1	FY+2
Salary			
Equipment/Facilities			
Supplies			
Total			

Report Document

Report Document - Text Analysis

Report Document - Text Analysis

Appendix Documents

2. Thank You

E-mail user

Apr 15, 2016 11:15:33 Success: Email Sent to: amw@purdue.edu